# Study of the effect of Mn doping on the $BiFeO_3$ system



2007 J. Phys.: Condens. Matter 19 136202

(http://iopscience.iop.org/0953-8984/19/13/136202)

IOP PUBLISHING JOURNAL OF PHYSICS: CONDENSED MATTER

J. Phys.: Condens. Matter **19** (2007) 136202 (8pp) doi:10.1088/0953-8984/19/13/136202

# Study of the effect of Mn doping on the $BiFeO_3$ system

**Deepti Kothari[1], V Raghavendra Reddy[1,4], Ajay Gupta[1], D M Phase[1], N Lakshmi[2], S K Deshpande[3] and A M Awasthi[1]**

[1] UGC-DAE Consortium for Scientific Research, Khandwa Road, Indore-452017, India
[2] Department of Physics, M L Sukhadia University, Udaipur-313001, India
[3] UGC-DAE Consortium for Scientific Research, R-5 Shed, BARC, Trombay, Mumbai-400085, India

E-mail: vrreddy@csr.ernet.in and varimalla@yahoo.com

Received 30 November 2006, in final form 7 February 2007
Published 12 March 2007
Online at stacks.iop.org/JPhysCM/19/136202

**Abstract**

In this work a Mn doped magnetoelectric $BiFeO_3$ system is studied. X-ray diffraction (XRD), scanning electron microscopy, energy dispersive x-ray analysis (EDX), Mössbauer spectroscopy at room and high temperatures, differential scanning calorimetry (DSC), high temperature magnetization, dielectric constant measurements and x-ray photoelectron spectroscopy (XPS) are used to characterize the samples. The XRD result shows $BiFeO_3$ as a major phase along with about 1–2% impurity phase. EDX shows the equi-atomic ratio of Bi and Fe site cations. Using DSC it is observed that the Néel temperature decreases with Mn doping. Using Mössbauer and XPS it is observed that Fe exists in the +3 oxidation state. The samples have an antiferromagnetic nature with Mn doping.

## 1. Introduction

Recently, multiferroic materials, which possess two or all three of the so-called ferroic properties, namely ferromagnetism, ferroelectricity and ferroelasticity, have become the focus of research [1]. Materials that simultaneously show electric and magnetic ordering are attracting much attention due to their promising multifunctional device applications and also because of their interesting physics. $BiFeO_3$ (BFO) is a commensurate ferroelectric ($T_c \sim 830\,^{\circ}C$) [2] and an incommensurate antiferromagnetic ($T_N \sim 370\,^{\circ}C$) [3] system at room temperature. However, from a technological point of view, the magnetoelectric material has to be either ferromagnetic or ferrimagnetic at room temperature. Due to the spiral magnetic structure [4] with long wavelength (∼62 nm), even weak ferromagnetism is not observed in $BiFeO_3$ and consequently no linear magnetoelectric effect. However, the linear magnetoelectric

[4] Author to whom any correspondence should be addressed.

effect is reported with the application of large magnetic fields [5], chemical substitutions [6] and epitaxial strains in the case of thin films [7]. It has been predicted that spontaneous magnetization can be induced in $BiFeO_3$ either by changing the Fe–O–Fe bond angle or by a statistical octahedral distribution of Fe with mixed valence and chemical substitution [1]; in the case of thin films, however, it has been shown that heteroepitaxially strained BFO films become ferromagnetic at room temperature and show a remarkably large magnetoelectric effect [8]. Recently, room temperature ferromagnetism and ferroelectricity were reported in $Bi_{1-x}Ba_xFeO_3$ system [9]. Charge compensation with the Ba doping requires the formation of either $Fe^{4+}$ or oxygen vacancies and it is concluded that the statistical distribution of $Fe^{4+}$ and $Fe^{3+}$ is the reason for the net magnetization and ferromagnetism in Ba doped BFO. Palkar *et al* have studied Mn doped $BiFeO_3$ with the intention that the substituted Mn will introduce a mixed valence of Fe (i.e. $Fe^{3+}$ and $Fe^{2+}$), and concluded that the Mn substitution does not introduce ferromagnetism into the system [10]. The Mn substituted BFO thin films are shown to have better properties in terms of leakage current density [11]. Surprisingly, in all the above studies no effort was made to study the oxidation state of Fe (with the chemical substitution). The aim of the present work is to study the oxidation state of Fe, which is expected to throw light on the mechanism of the magnetic properties of BFO when it is attempted to change the magnetic properties with chemical substitution. Mössbauer spectroscopy, an ideal technique for studying the hyperfine interactions of Fe in a given compound, and x-ray photoelectron spectroscopy are used for this purpose.

## 2. Experimental details

Three samples with the composition $La_{0.1}Bi_{0.9}Fe_{1-x}Mn_xO_3$ (with $x = 0$, 5 and 10% henceforth designated as Mn0, Mn5 and Mn10, respectively) are prepared through solid-state reaction as described by Mahesh Kumar *et al* [12]. The small amount of La is added to stabilize the perovskite phase of $BiFeO_3$ [13] and it is reported that the addition of a small amount of La does not affect the ferroelectric properties of $BiFeO_3$ [14]. The x-ray diffraction (XRD) measurements were carried out with Cu K$\alpha$ radiation using a Rigaku powder diffractometer equipped with a rotating anode x-ray generator with 40 kV and 100 mA power settings. Modulated differential scanning calorimetry was used to study the variation in the antiferromagnetic (AFM) to paramagnetic (PM) transition temperature with Mn doping. The Mössbauer measurements were carried out using a standard PC-based spectrometer equipped with a Weissel velocity drive operating in the constant acceleration mode. Mössbauer measurements at high temperatures were carried out using an Austin vacuum furnace. The x-ray photoelectron spectroscopy (XPS) study was carried out using an Omicron EA-125 photoelectron spectrometer at a base pressure better than $5 \times 10^{-10}$ Torr. Al K$\alpha$ radiation was employed for the analysis, with the source operated at an emission current of 10 mA and an anode voltage of 10 kV. A concentric hemispherical energy analyser with 50 eV pass energy giving an overall resolution of 0.8 eV was used. Au $4f_{7/2}$ at 84.7 eV served as an external reference. To correct the shifts in binding energies of core levels due to the charging effect, the graphitic C 1s peak at 284.7 eV was used as an internal reference. Energy dispersive x-ray fluorescence (EDX) analysis was carried out using an Oxford EDS spectrometer (INCA) installed on a JEOL JSM 5600 system to determine the chemical composition of the prepared samples. The high temperature susceptibility measurements were carried out using a Lakeshore 7400 series vibrating sample magnetometer (VSM) in a field of 50 Oe. The dielectric constant as a function of frequency and temperature was measured using HP4194A impedance/gain-phase analyser.

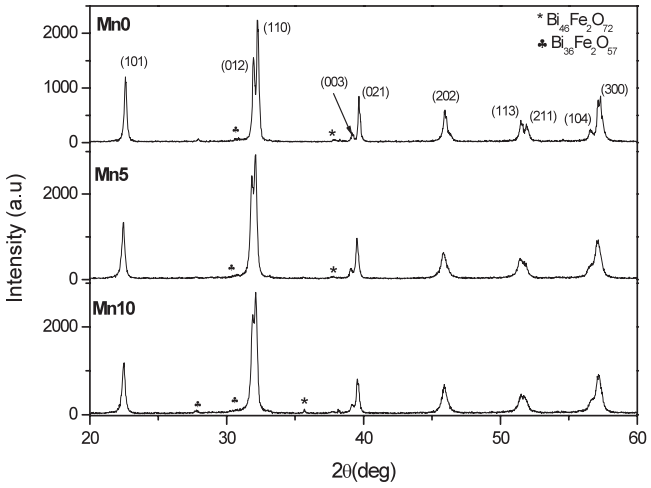


**Figure 1.** X-ray diffraction patterns of Mn0, Mn5 and Mn10 samples.

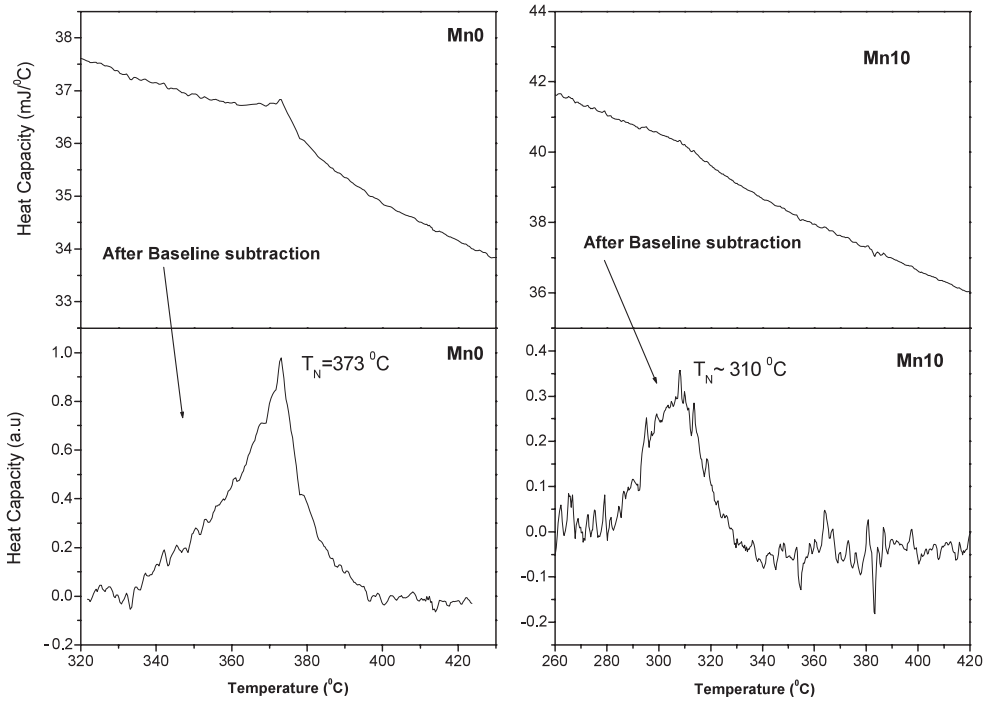


**Figure 2.** DSC curves of Mn0 and Mn10 samples showing the antiferromagnetic to paramagnetic transition.

## 3. Results and discussion

Figure 1 shows the XRD measurements of the three samples. The parent compound BFO has a distorted perovskite rhombohedral structure. From the XRD it is clear that with the Mn doping $La_{0.1}Bi_{0.9}Fe_{1-x}Mn_xO_3$ has a majority phase $BiFeO_3$ crystallization. Because of the

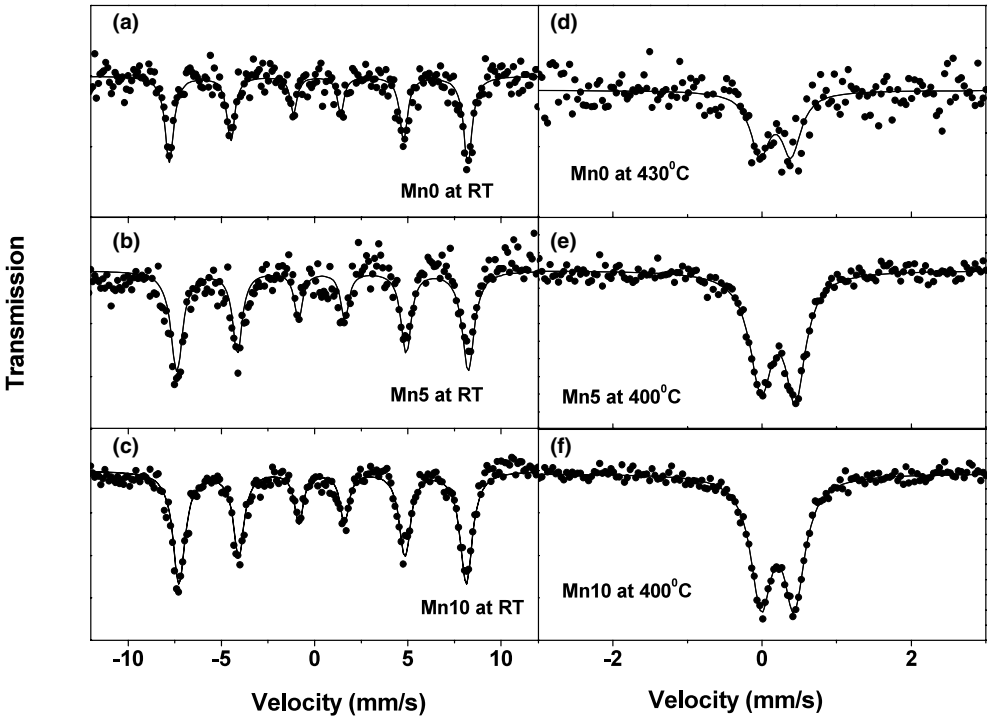


**Figure 3.** (a)–(c) The Mössbauer spectra of Mn0, Mn5 and Mn10 samples, respectively, at room temperature. (d)–(f) The Mössbauer spectra of Mn0, Mn5 and Mn10 samples, respectively, at 430, 400 and 400 °C.

kinetics of formation, a mixture of $BiFeO_3$ as a major phase along with other impurity phases is always obtained during synthesis. Several authors have reported the existence of $Bi_{46}Fe_2O_{72}$, $Bi_{36}Fe_2O_{57}$, and $Bi_2Fe_4O_9$ as impurity phases [15]. In the present study, the concentration of such impurity phases is about 2% compared to the intense peak of $BiFeO_3$. EDX analysis of all the samples indicated that the samples are chemically homogeneous with the ratio of Bi and Fe site cations being close to 1. Figure 2 shows the DSC measurement of the Mn0 ($La_{0.1}Bi_{0.9}FeO_3$) and Mn10 ($La_{0.1}Bi_{0.9}Fe_{0.9}Mn_{0.1}O_3$) samples. An apparent decrease in the heat capacity at high temperatures is due to the contribution from the sample holder, and hence for the sake of clarity a base line is subtracted from the data and the resulting data are shown in figure 2. Clear peaks due to the AFM to PM transition are seen in both the samples. The $T_N$ obtained (∼373 °C) for Mn0 matches well with the reported value for BFO. It is observed that $T_N$ decreases with the Mn doping and the observed value is ∼310 °C in the case of Mn10. In fact, the reduction of $T_N$ to near room temperature with Mn doping is used to give large magnetoelectric effects at room temperature [16]. The FE to PE transition could not be observed due to the limitations of the instrument as the FE to PE transition is expected to be above 800 °C. In addition to the decrease in magnetic transition temperature with Mn doping, it is observed that the peak width increased, indicating the associated broad transition in the Mn10 sample.

Figures 3(a)–(c) show the room temperature (RT) Mössbauer measurements of the three samples. The poor statistics even after few days of data acquisition is due to the presence of high-$Z$ elements such as Bi and La in the samples. In fact, due to the fact that Bi has

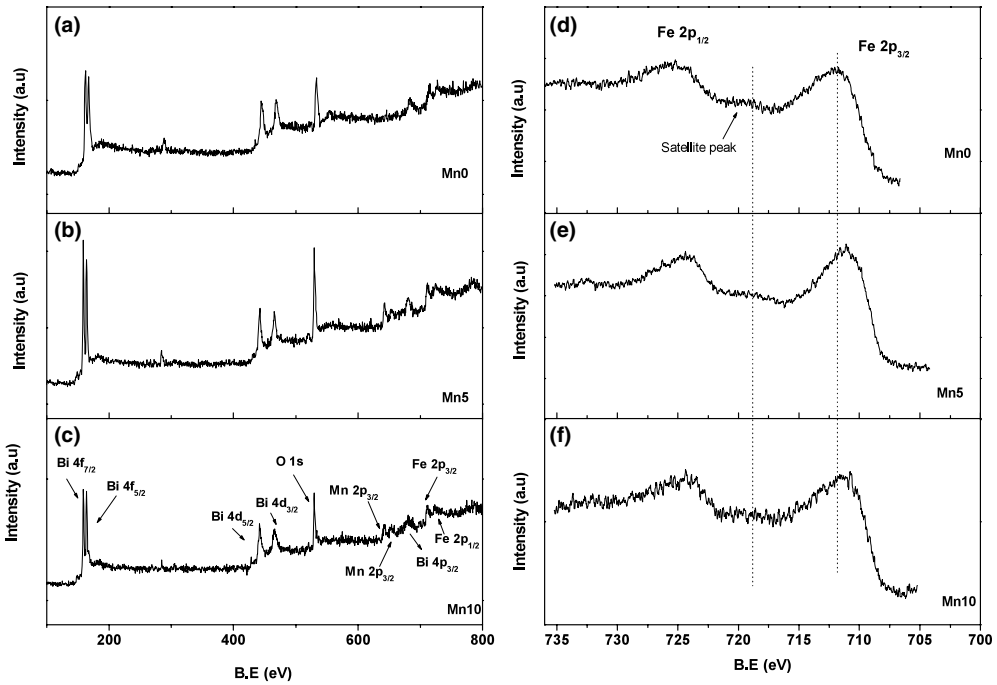


**Figure 4.** (a)–(c) XPS spectroscopy survey scans of Mn0, Mn5 and Mn10 samples, respectively. (d)–(f) XPS scans of Fe 2p region of Mn0, Mn5 and Mn10 samples, respectively. The dotted lines show the satellite peak confirming the $Fe^{3+}$ state and the shift in the binding energy with Mn doping.

a very high absorption coefficient for 14.4 keV Mössbauer $\gamma$-rays, Blauuw *et al* used $^{57}$Fe enrichment for the Mössbauer study [17]. The magnetic hyperfine splitting spectra measured at room temperature of all three samples indicate that the Nèel temperatures are above RT, consistent with the DSC data. The data are fitted with the NORMOS-SITE program and the obtained parameters are with respect to natural iron. The hyperfine field is observed to decrease from 49.59 $\pm$ 0.06 to 47.76 $\pm$ 0.05 T with 10% Mn doping for the RT spectra. Using neutron diffraction measurements Sosnowska *et al* reported a decrease in the average magnetic moment due to some kind of local magnetic disorder in $BiFe_{0.8}Mn_{0.2}O_3$ [18]. The decrease in the hyperfine field with Mn doping might also be from local magnetic disorder. But, the Mössbauer spectra data at RT did not show the presence of any $Fe^{2+}$, which one would expect if the substituted Mn exists in the +4 state and as a result of charge compensation. The obtained isomer shift value indicates the Fe to be in the +3 oxidation state even in the Mn10 sample.

Since the hyperfine field of $Fe^{2+}$ is not appreciably different from that of $Fe^{3+}$, the presence of $Fe^{2+}$ might thus be contributing to the broadening of the lines with Mn doping [19]. The line width is found to increase from 0.540 $\pm$ 0.037 to 0.769 $\pm$ 0.021 mm s$^{-1}$ for RT spectra with 10% Mn doping. To check whether the presence of $Fe^{2+}$ is contributing to the line broadening, the Mössbauer spectra of all the samples were taken above $T_N$ in the paramagnetic region. Figures 3(d)–(f) show the high temperature Mössbauer measurements for the three samples. A clear single doublet with isomer shift values of 0.179 $\pm$ 0.016, 0.216 $\pm$ 0.005 and 0.209 $\pm$ 0.002 mm s$^{-1}$, respectively, for Mn0, Mn5 and Mn10 corresponding to $Fe^{3+}$ is observed. The apparent decrease in the isomer shift is due to the second-order Doppler

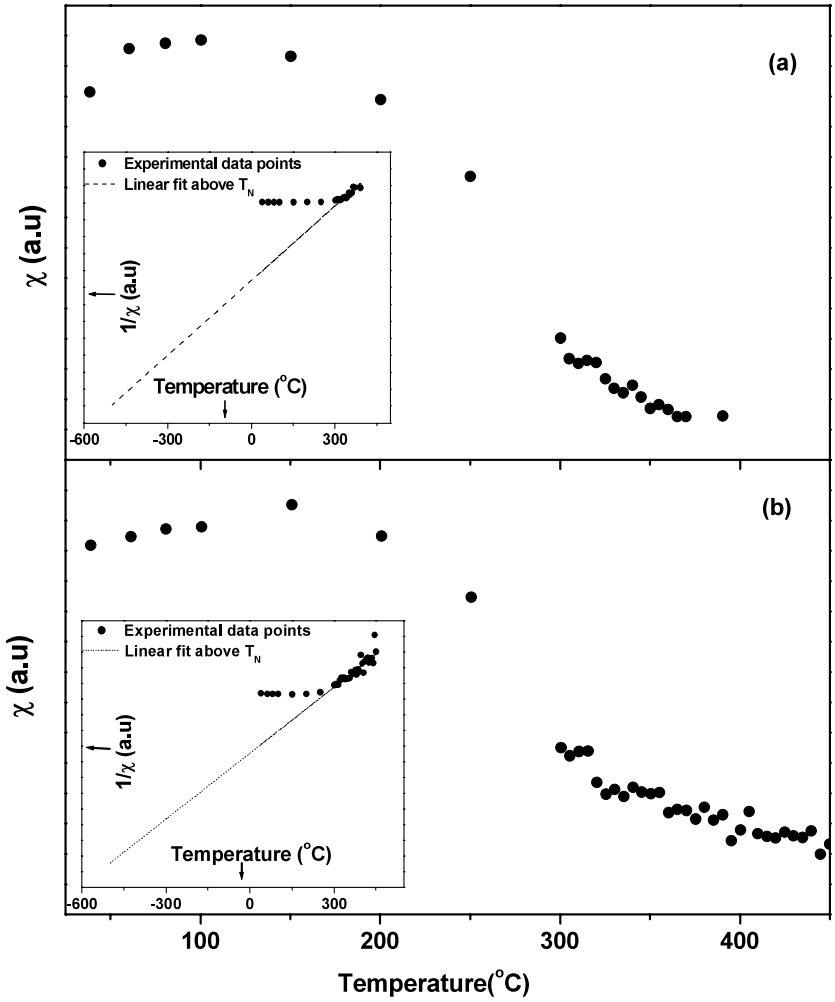


**Figure 5.** (a), (b) The temperature dependence of susceptibility ($\chi$) of Mn0 and Mn5 samples. The inset shows the linear fit of the $1/\chi$ data above $T_N$. Note the negative intercept of the extrapolated curve.

shift [20]. Therefore, from the Mössbauer results one can conclude that with Mn doping no multiple oxidation states of Fe, i.e. $Fe^{2+}$ and $Fe^{3+}$, is observed.

XPS measurements were performed on these samples to check the oxidation states of Fe. The survey scans for three samples are shown in figures 4(a)–(c). From the spectrum one can see the peaks coming from La, Bi, Fe, O and Mn in the case of Mn5 and Mn10 samples, thus confirming the chemical composition of the samples. After taking the survey scan, a narrow range scan was done for Fe 2p. The carbon peak was also scanned for the compensation of charging effect. Figures 4(d)–(f) show the Fe 2p photoelectron spectra obtained for the three samples. It is reported that Fe 2p photoelectron peaks from oxidized iron are associated with satellite peaks [21]. In principle, the satellite peak with the main peak appears due to two final states caused by photoemission of the Fe site of the oxide. In one of the final states, a significant amount of charge transfer took place in the valence band from ligand (oxygen) site to metal ($Fe^{x+}$) site in the relaxation process after the photo-excitation. As the $Fe^{2+}$ and

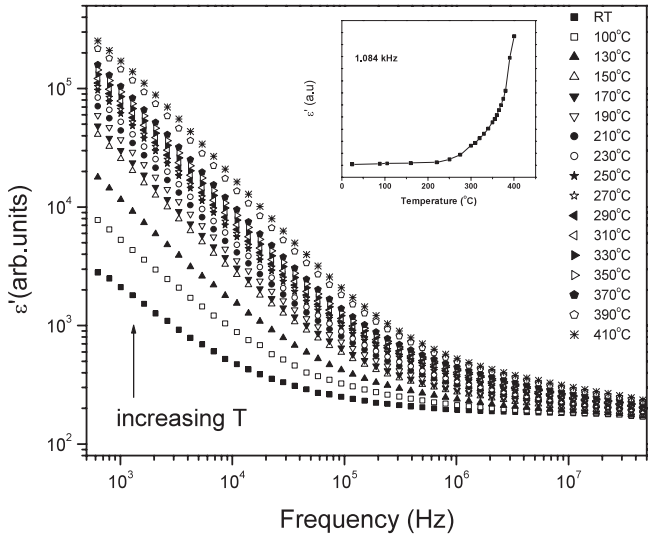


**Figure 6.** The dielectric constant as a function of frequency for the Mn0 sample. The temperature is increased from room temperature. The inset shows the variation of dielectric constant with temperature at 1.084 kHz.

$Fe^{3+}$ states have d6 and d5, respectively, in the valence band, the satellite peak appeared at different positions during relaxation of the metal ion and was observed to be characteristic of the oxidation state of iron. The analysis of the Fe $2p_{3/2}$ photoelectron peak for different chemical states of Fe is complicated due to the huge background. But the satellite peaks for $Fe^{3+}$ and $Fe^{2+}$ are found to be important for identifying the chemical states. The $Fe^{2+}$ $2p_{3/2}$ peak at 709.5 eV is always associated with a satellite peak at 6.0 eV above the principal peak, whereas the $Fe^{3+}$ $2p_{3/2}$ peak at 711.2 eV is associated with a satellite peak at 8.0 eV [21]. The binding energy of the Fe $2p_{3/2}$ peak for Mn0 is 711.8 eV with a satellite peak at about 8.0 eV above the principal peak, which confirms the presence of $Fe^{3+}$. With Mn doping the binding energy values of Fe $2p_{3/2}$ were observed to be 711.06 and 710.63 eV, respectively, for Mn5 and Mn10. But, with the Mn doping the distinct satellite peaks were also observed at around 8.0 eV above the main peak. Thus in the present case the reduction of the main peak position to 710.63 eV in Mn10 is not due to the presence of the $Fe^{2+}$ state as the distinct characteristic satellite peak at around 8.0 eV above the principal peak confirmed the presence of only the $Fe^{3+}$ state [22]. These results are consistent with the Mössbauer measurements discussed above.

In addition to the electronic structure measurements discussed above, few representative magnetic and dielectric measurements are shown in the present work. The high temperature magnetization measurements are shown in figure 5. The initial cusp in the susceptibility is not clearly seen in the measurements, but the linear part of $1/\chi$ above the $T_N$ and its extrapolation to a negative temperature at $1/\chi = 0$ (shown in the inset of figure 5) clearly confirms the antiferromagnetic nature of the samples [23]. The observed antiferromagnetic nature of the samples is in accordance with the results of Palkar *et al* [10]. Figure 6 shows the dielectric constant measurements of the Mn0 sample as a function of frequency and temperature. It is observed that the dielectric constant decreases with increasing frequency, which is explained by the phenomenon of dipole relaxation wherein at low frequencies the dipoles are able to follow the frequency of the applied field [9, 15].

In conclusion, we have studied the magnetoelectric $La_{0.1}Bi_{0.9}Fe_{1-x}Mn_xO_3$ (with $x = 0, 5$ and 10%) system using Mössbauer and XPS measurements to find the Fe oxidation state. The measurements indicate that Fe exists in the +3 oxidation state with even 10% Mn doping, and hence Mn substitution does not introduce any mixed valence in the system and consequently ferromagnetism.

## References


[1] Prellier W, Singh M P and Murugavel P 2005 *J. Phys.: Condens. Matter* **17** R803
Eerenstein W, Mathur N D and Scott J F 2006 *Nature* **442** 759
Fiebig M 2005 *J. Phys. D: Appl. Phys.* **38** R123
[2] Kubel F and Schmid H 1990 *Acta Crystallogr.* B **46** 698
[3] Fischei P, Polemska M, Sosnowska I and Szymanski M 1980 *J. Phys. C: Solid State Phys.* **13** 1931
[4] Sosnowska I, Lowenhaupt M, David W I F and Ibberson R M 1992 *Physica* B **180/181** 117
[5] Popov Y F, Kadomtseva A M, Vorob'ev G P and Zvezdin A K 1994 *Ferroelectrics* **162** 135
[6] Murashov V A, Rakov D N, Ionov V M, Dubenko I S, Titov Y V and Gorelik V S 1994 *Ferroelectrics* **162** 11
[7] Bai F, Wang J, Wang M, Li J, Wang N, Pyatakov A P, Zvezdin A K, Cross L E and Viehland D 2005 *Appl. Phys. Lett.* **86** 32511
[8] Wang J, Neaton J B, Zheng H, Nagarajan V, Ogale S B, Liu B, Viehland D, Vaithyanathan V, Schlom D G, Waghmare U V, Spaldin N A, Rabe K M, Wuttig M and Ramesh R 2003 *Science* **299** 1719
[9] Wang D H, Goh W C, Ning M and Ong C K 2006 *Appl. Phys. Lett.* **88** 212907
[10] Palkar V R, Kundaliya D C and Malik S K 2003 *J. Appl. Phys.* **93** 4337
[11] Singh S K, Ishiwara H and Maruyama K 2006 *Appl. Phys. Lett.* **88** 262908
Kim J K, Kim S S, Choi E J, Kim W J, Bhalla A S and Song T K 2006 *J. Korean Phys. Soc.* **49** S566
[12] Mahesh Kumar M, Palkar V R, Srinivas K and Suryanarayana S V 2000 *Appl. Phys. Lett.* **76** 2764
[13] Palkar V R, Kundaliya D C, Malik S K and Bhattacharya S 2004 *Phys. Rev.* B **69** 212102
[14] Sosnowska I, Peterlin-Neumaier T and Steichele E 1982 *J. Phys. C: Solid State Phys.* **15** 4835
[15] Kumar M and Yadav K L 2006 *J. Appl. Phys.* **100** 74111
Kumar M and Yadav K L 2006 *J. Phys.: Condens. Matter* **18** L503 and references therein
[16] Yang C H, Koo T Y and Jeong Y H 2005 *Solid State Commun.* **134** 299
[17] Blaauw C and van der Woude F 1973 *J. Phys. C: Solid State Phys.* **6** 1422
[18] Sosnowska I *et al* 2000 *Physica* B **276–278** 576
[19] Shirane G, Cox D E, Takei W J and Ruby S L 1962 *J. Phys. Soc. Japan* **17** 1598
[20] Greenwood N N and Gibb T C 1971 *Mössbauer Spectroscopy* (London: Chapman and Hall)
[21] Wandelt C 1982 *Surf. Sci. Rep.* **2** 1
[22] Mittal V K *et al* 2006 *Solid State Commun.* **137** 6
[23] Cullity B D 1972 *Introduction to Magnetic Materials* (Reading, MA: Addison-Wesley)